

**Thermal conductivity in amorphous ices from molecular dynamics**Niall J. English,<sup>1,\*†</sup> John S. Tse,<sup>2,\*‡</sup> and Rory Gallagher<sup>1</sup><sup>1</sup>*The SEC Strategic Research Cluster and the Centre for Synthesis and Chemical Biology, School of Chemical and Bioprocess Engineering, University College Dublin, Belfield, Dublin 4, Ireland*<sup>2</sup>*Department Physics and Engineering Physics, University of Saskatchewan, Saskatoon, Saskatchewan, Canada S7N 5E2*

(Received 23 July 2010; published 2 September 2010)

The observed unusual thermal conductivities of low-, high- and very high-density amorphous ices (*a*-ices, LDA, HDA, and VHDA) are reproduced by equilibrium molecular-dynamics calculations with the Green-Kubo approach. The fast and slow relaxation times of the heat flux correlation functions were found to be dependent on, respectively, the short- and intermediate-range structural ordering. In conjunction with the collective nature of the acoustic vibrations, it can be concluded that the short and intermediate ordering of *a*-ices is similar to collapsed ice rather than a liquid. The larger phonon linewidths in HDA and VHDA vis-à-vis LDA are a clear indication of hybridization between acoustic and optic phonon branches resulting in an increase in decay channels in the dense amorphous states and shorter phonon mean-free paths.

DOI: [10.1103/PhysRevB.82.092201](https://doi.org/10.1103/PhysRevB.82.092201)

PACS number(s): 65.60.+a, 63.20.Pw, 65.20.De

Polymorphism of water is a prevailing model to rationalize the anomalous properties of liquid and supercooled water,<sup>1,2</sup> based on the observation of low-temperature pressure-induced amorphization of crystalline ice, leading to high-density amorphous ice (*a*-ice, HDA) formation.<sup>3</sup> Subsequent studies<sup>4,5</sup> have revealed new classes of *a*-ice, which, depending on thermodynamic conditions, may exhibit different properties. For example, a low-density amorphous (LDA) form is formed upon heating HDA at ambient pressure.<sup>3,4</sup> Under pressure, an even very high-density amorphous (VHDA) form may be obtained by heating HDA.<sup>5</sup> It is conjectured that *a*-ice polymorphs and liquid water may be thermodynamically connected. This has led to the hypothesis of the two-liquid model for water and the prediction of a second critical point.<sup>1</sup> Numerous experimental and theoretical investigations to test this hypothesis have led to conflicting results; a definitive conclusion is still elusive. An outstanding issue is the relationship between liquid water and LDA and HDA. It is recognized that water and HDA share some structural similarities.<sup>6</sup> However, despite their amorphous nature, LDA, HDA,<sup>7</sup> and VHDA (Ref. 8) exhibit crystal-like phonon dispersion. This is supported by the crystal-like temperature profile of LDA thermal conductivity.<sup>9,10</sup> In contrast, HDA and VHDA thermal conductivities are almost identical with only a very weak, amorphouslike, temperature dependence. This suggests strongly the short- and intermediate-range structural orders of *a*-ices may be similar to the crystalline state but lack long-range correlation. If these were correct, then *a*-ices are structurally and thermodynamically closer to underlying crystalline ice polymorphs than the liquid state. A microscopic understanding of the mechanisms of thermal conduction and phonon dispersion of *a*-ices is therefore essential. This study aims to (i) use atomistic molecular dynamics (MD) to predict thermal conductivities of ice *Ih*, LDA, HDA, and VHDA in their respective stability regions, and (ii) investigate mechanisms of thermal conduction and phonon propagation from simulation results.

The thermal conductivity ( $k$ ) was evaluated via the Green-Kubo method,<sup>11</sup> integrating the heat flux vector ( $\mathbf{J}$ ) autocorrelation function (JACF),  $k = \frac{V}{3k_B T^2} \int_0^\infty \langle \mathbf{J}(t) \cdot \mathbf{J}(0) \rangle dt$ , from microcanonical-ensemble MD calculations and neglecting quantum effects, as described in previous work<sup>12,13</sup> and the supplementary information.<sup>14</sup> The TIP4P-Ice<sup>15</sup> water model, parametrized explicitly for crystalline and amorphous ice, was used. For ice *Ih*, simulations were performed at 30 K, 100 K, 150 K, and 200 K and 1 bar, and for LDA, HDA, and VHDA, at 0.1 GPa, 0.8 GPa, and 1.1 GPa, respectively (in accord with experimental pressures), at 30 K, 50 K, 80 K, 110 K, 140 K, and 180 K. The computed thermal conductivities reproduce clearly experimental trends<sup>9,10</sup> [cf. Fig. 1(a)]. For LDA, the crystal-like behavior of increasing conductivity with decreasing temperature is predicted. Within numerical error, the conductivities of HDA and VHDA are very similar, with VHDA slightly higher, and exhibit little variation with temperature. The theoretical values are also in semiquantitative agreement with observed results.<sup>9,10</sup> A quantitative agreement between theory and experiment is not anticipated. This is due partly to empirical potentials' shortcomings and inherent experiment errors due to sample quality and boundary scatterings. For this study's purposes, the agreement with experiment indicates the calculations' reliability.

The heat flux correlation function exhibits damped oscillations. The oscillatory features correspond to the rapid transport of energy back and forth over microscopic distances by lattice vibrations. For a monatomic solid where only acoustic phonons are present, the JACF is characterized by a fast relaxation process followed by a slow decay.<sup>16</sup> In molecular solids, there is an additional term from optic phonons.<sup>17</sup> These relaxation times, related to energy-transfer times by phonons, may be extracted by fitting JACFs to sums of exponentially decaying functions, with cosine-modulated terms for optic component decay,<sup>12,13,17</sup> i.e.,

$$\begin{aligned}
 \text{JACF}(t) = & \sum_{i=1}^{n_{ac}} A_i \exp(-t/\tau_i) + \sum_{j=1}^{n_{opt}} \\
 & \times \left[ \sum_{k=1}^{n_{o,j}} B_{jk} \exp(-t/\tau_{jk}) \right] \cos \omega_{0,j}t \\
 & + \sum_{j=1}^{n_{opt}} C_j \cos \omega_{0,j}t. \quad (1)
 \end{aligned}$$

The first term consists of short- and long-range acoustic relaxation times. The second and third terms account for contributions from optic phonons, modulated by cosine terms for optic component decay.<sup>12,13,17</sup> The fitting procedure is explained in previous work.<sup>12,13</sup> The relaxation times, parameters and terms' contributions to the overall thermal conductivity are provided in Table S-I.<sup>14</sup> A summary highlighting only relevant parameters at the minimum and maximum temperatures considered is in Table I. The relaxation times' temperature dependence is shown in Figs. 1(b) and 1(c).

Several characteristic features are evident from the results. The relaxation times for ice *Ih* and LDA are very similar, as well as between HDA and VHDA. The short- and long-range acoustic relaxation times,  $\tau_{sh,ac}$  and  $\tau_{lg,ac}$ , are temperature dependent but are shorter for HDA and VHDA than for LDA and ice *Ih*. A surprising but distinct observation is that the contribution of the optic modes to the conductivity is substantially larger (approximately 30% and almost double) for HDA and VHDA than LDA and ice *Ih*. Generally, optic phonons are expected not to contribute significantly to the thermal conductivity in crystalline solids.<sup>18</sup> This can be explained qualitatively from the viewpoint of short and intermediate orders in the ice structures. From structural studies, it is already known that the structure of LDA is similar to ice *Ih*.<sup>6</sup> However, the HDA and VHDA structures are quite different.<sup>6</sup> In HDA, a water molecule occupies the interstitial site.<sup>6</sup> In VHDA, akin to ice VI, a second water was inserted in interstitial sites.<sup>6</sup> These interstitial waters do not disrupt hydrogen (h-) bond network connectivity or create additional h-bonds but distort the waters' local environment.

The phonon relaxation time is a measure of the fluctuation of the phonon occupation number from its equilibrium value. The average long-range acoustic relaxation time,  $\tau_{lg,ac}$ , first derived by Peierls,<sup>19,20</sup> is due to heat flux fluctuation by the anharmonic potential and is a simplification of the exact Green-Kubo result.<sup>16</sup> A small  $\tau_{lg,ac}$  indicates strong dephasing (scattering) of propagating phonons by anharmonicity, leading to a rapid decay. This effect is directly related to the solid's intermediate- and long-range structures. The origin of the short acoustic relaxation time,  $\tau_{sh,ac}$ , is still uncertain. At thermodynamic equilibrium, energy fluctuations create instantaneous, localized "hot" spots. It is reasonable to propose  $\tau_{sh,ac}$  represents the temporal exchange of energy pockets with immediate surroundings prior to heat transport away by lattice vibrations (i.e.,  $\tau_{lg,ac}$ ). Therefore, this effect is influenced mostly by the immediate environment. In view of regular four-coordinated water sites in ice *Ih* and LDA, it is expected that energy transfer between nearest-neighbor wa-

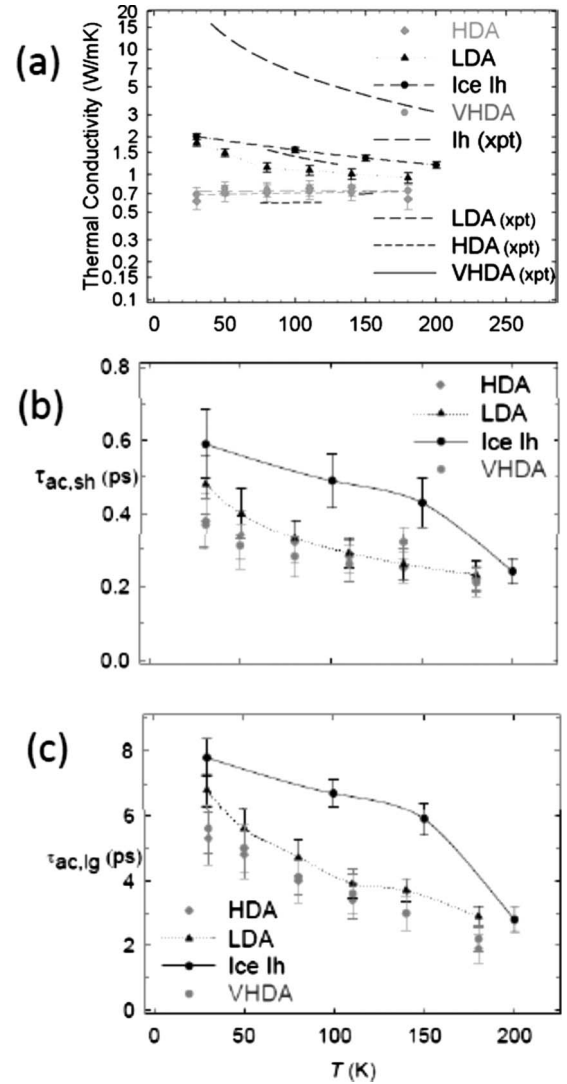


FIG. 1. (a) Thermal conductivity, and (b) short- and (c) long-range acoustic relaxation times,  $\tau_{sh,ac}$  (top) and  $\tau_{lg,ac}$  (bottom), for *Ih*, LDA, VHDA, and HDA structures at 1 bar, and 0.1 GPa, 1.1 GPa, and 0.8 GPa, respectively. In (a), fits to the experimental data for thermal conductivity are shown for their region of applicability (Ref. 10).

ters is facilitated more than in distorted environment of HDA and VHDA. Thus,  $\tau_{sh,ac}$  are similar between LDA and ice *Ih* and longer than in HDA/VHDA. The crystalline(like) long-range structures of ice *Ih* and LDA suggest anharmonicity in the potential will be weaker than HDA and VHDA, reflected by shorter  $\tau_{lg,ac}$  in the latter two cases.

The larger contribution of optic phonons to thermal conductivity merits more detailed investigation; the dynamical structure factor,  $S(k, \omega)$ ,<sup>11</sup> was computed at 80 K for momentum transfers  $k=0.2, 0.35, \text{ and } 0.5 \text{ \AA}^{-1}$  for LDA, HDA, and VHDA (cf. Fig. 2). In all cases, the crystal-like phonon dispersion observed in inelastic x-ray scattering (IXS) experiments<sup>7,8</sup> was predicted, in marked contrast to essentially no dispersion in  $S(k, \omega)$  for liquid water (in accord with IXS experiments—see Fig. S1 in the supplementary material for liquid water results<sup>14</sup>). The positions of the phonon bands and the linewidths extracted by fitting  $S(k, \omega)$  with Lorentz-

TABLE I. Relaxation times and terms' contributions to the overall predicted thermal conductivity (see Table S-I for more detail).

Type	$T$ (K)	$\tau_{sh,ac}$ (ps)	$\kappa_{sh,ac}$	$\tau_{lg,ac}$ (ps)	$\kappa_{sh,ac}$	$\kappa_{optic}$	$\kappa_{total}$	$\kappa_{optic}/\kappa_{total}$
lh	30	$0.59 \pm 0.094$	0.37	$7.8 \pm 0.56$	1.41	0.23	$2.01 \pm 0.11$	0.11
	200	$0.24 \pm 0.034$	0.21	$2.8 \pm 0.38$	0.82	0.16	$1.19 \pm 0.072$	0.13
HDA	30	$0.38 \pm 0.075$	0.18	$5.3 \pm 0.82$	0.25	0.18	$0.61 \pm 0.06$	0.27
	180	$0.22 \pm 0.036$	0.37	$1.9 \pm 0.44$	0.20	0.17	$0.64 \pm 0.06$	0.27
LDA	30	$0.48 \pm 0.08$	0.42	$6.8 \pm 0.51$	1.11	0.26	$1.79 \pm 0.12$	0.15
	180	$0.23 \pm 0.04$	0.24	$2.9 \pm 0.32$	0.55	0.15	$0.94 \pm 0.09$	0.16
VHDA	30	$0.37 \pm 0.070$	0.20	$5.6 \pm 0.76$	0.27	0.22	$0.69 \pm 0.07$	0.32
	180	$0.21 \pm 0.040$	0.32	$2.2 \pm 0.40$	0.22	0.20	$0.74 \pm 0.06$	0.27

ian functions are also essentially in agreement with experiments. At  $k=0.2, 0.35,$  and  $0.5 \text{ \AA}^{-1}$ , the respective principal phonon peaks (in  $\text{cm}^{-1}$ ) were found at (the corresponding experimental value specified thereafter in parentheses<sup>7,8</sup>): 38 (40), 62 (52), and 105 (95) for LDA; 44 (49), 64 (52), and 110 (97) for HDA; and 41 (40), 77 (72), and 75/135 (112) for VHDA. Note that the measurements for VHDA were performed on a deuterated sample.<sup>8</sup> The calculations reveal a nondispersive mode at  $\sim 40 \text{ cm}^{-1}$  that may correspond to the  $k$ -independent feature observed at  $\sim 72 \text{ cm}^{-1}$  in the VHDA spectra. The extracted linewidths also show a  $k^2$  dependence<sup>8</sup> (cf. Fig. 3); a significant observation is the linewidths for VHDA and HDA are larger than for LDA, and more so at large momentum transfer. In Peierls' approximation,<sup>16</sup> the thermal conductivity is  $\lambda = \frac{k_B}{V} \sum_i v_i^2 \tau_i$ , where  $v_i$  and  $\tau_i$  are the

velocity and relaxation time for the  $i$ th phonon group. The phonon lifetime is related to the linewidth ( $\Gamma=1/2\tau$ ). A larger linewidth means a shorter lifetime and a smaller contribution to the conductivity from that phonon. Since the velocities of sound are similar among  $a$ -ices, the larger HDA and VHDA phonon linewidths indicate the conductivity will be smaller. Larger linewidths in disordered systems have been suggested to be the result of hybridization between acoustic and optic phonon modes.<sup>21,22</sup> Mixing opens multiple decay channels for phonon excitations, thereby reducing lifetimes. This explanation is consistent with our observation (cf. Table I) that contributions from optic modes in HDA and VHDA are much more significant than in crystalline-like LDA. In passing, it has been pointed out that the large linewidth observed in a glassy material may be due to the large structural disorder as shown in a comparative study of the IXS between polycrystalline and glassy ethanol.<sup>24</sup> We believe that this is not to be the case here, since the calculated  $S(k, \omega)$  for  $a$ -ices and liquid water (see supplementary information) are significantly different. The persistence of crystal-like phonon dispersion is a clear reflection of short- and intermediate-range structural correlations in  $a$ -ices. In recent lattice dynamics calculations,<sup>23</sup> it has been shown that water molecules' collective vibrations extend throughout LDA and HDA and can involve up to 70% of all molecules. This is because the h-bond network is preserved in these disordered

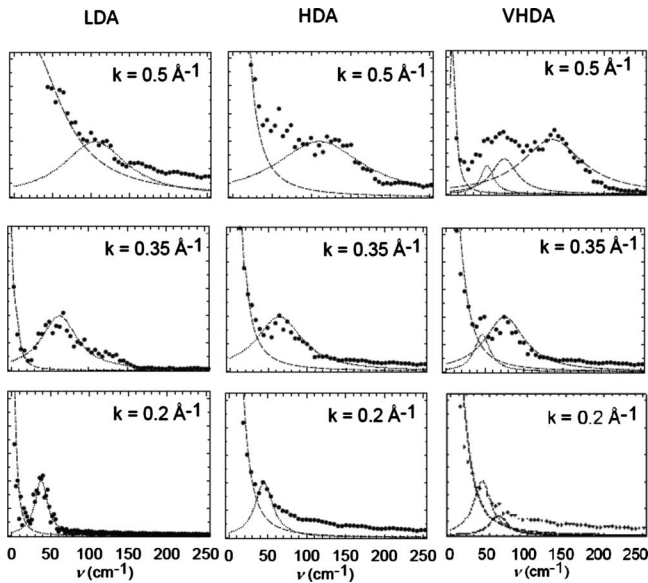


FIG. 2. Dynamical structure factor,  $S(k, \omega)$  at 80 K for LDA, VHDA, and HDA at respective pressures of 0.1, 1.1, and 0.8 GPa computed at  $k=0.2, 0.35,$  and  $0.5 \text{ \AA}^{-1}$ . The curves under  $S(k, \omega)$  are fitted Lorentzian functions.

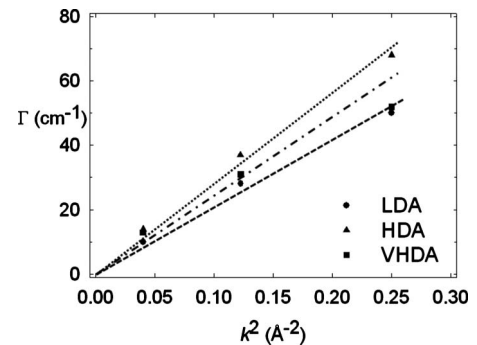


FIG. 3. Linewidth of the main peak in  $S(k, \omega)$  at 80 K and the same pressures as Figs. 1 and 2 as a function of  $k^2$  for LDA, HDA, and VHDA. The straight lines are guides to the eye.

structures, and this plays a significant role in their dynamical behavior.

The inconsistency of the temperature dependence of the conductivity in *a*-ices vis-à-vis typical disordered solids has been elucidated. In *a*-ices, the h-bond network's connectivity remains intact, and leads to crystal-like collective excita-

tions. The lower conductivities in HDA and VHDA manifest the proposed hybridization of acoustic and optic modes.<sup>21,22</sup> This study provides deeper insights into phonon propagation in materials with short- and intermediate-range structural disorders, an obvious consequence of the distinctive structures of *a*-ices vis-à-vis the nonpropagating nature of liquid water.

\*Corresponding author.

<sup>†</sup>niall.english@ucd.ie

<sup>‡</sup>john.tse@usask.ca

- <sup>1</sup>O. Mishima and H. E. Stanley, *Nature (London)* **396**, 329 (1998).
- <sup>2</sup>P. G. Debenedetti and H. E. Stanley, *Phys. Today* **56**(6), 40 (2003).
- <sup>3</sup>O. Mishima, L. D. Calvert, and E. Whalley, *Nature (London)* **310**, 393 (1984).
- <sup>4</sup>O. Mishima, L. D. Calvert, and E. Whalley, *Nature (London)* **314**, 76 (1985).
- <sup>5</sup>T. Loerting, C. Salzmann, I. Kohl, E. Mayer, and A. Hallbrucker, *Phys. Chem. Chem. Phys.* **3**, 5355 (2001).
- <sup>6</sup>J. L. Finney, A. Hallbrucker, I. Kohl, A. K. Soper, and D. T. Bowron, *Phys. Rev. Lett.* **88**, 225503 (2002).
- <sup>7</sup>H. Schober, M. M. Koza, A. Tölle, C. Masciovecchio, F. Sette, and F. Fujara, *Phys. Rev. Lett.* **85**, 4100 (2000).
- <sup>8</sup>M. M. Koza, B. Geil, M. Scheuermann, H. Schober, G. Monaco, and H. Requardt, *Phys. Rev. B* **78**, 224301 (2008).
- <sup>9</sup>O. Andersson and H. Suga, *Phys. Rev. B* **65**, 140201 (2002).
- <sup>10</sup>O. Andersson and A. Inaba, *Phys. Chem. Chem. Phys.* **7**, 1441 (2005).
- <sup>11</sup>D. J. Evans and G. P. Morriss, *Statistical Mechanics of Nonequilibrium Liquids* (Academic Press, San Diego, 1990).
- <sup>12</sup>N. J. English and J. S. Tse, *Phys. Rev. Lett.* **103**, 015901 (2009).

<sup>13</sup>N. J. English, J. S. Tse, and D. J. Carey, *Phys. Rev. B* **80**, 134306 (2009).

<sup>14</sup>See supplementary material at <http://link.aps.org/supplemental/10.1103/PhysRevB.82.092201> for expanded discussion of methodology, density calculations, full table of fitted parameters from JACF fits, and results for thermal conductivity and dynamical structure factor of liquid water.

- <sup>15</sup>J. L. F. Abascal, E. Sanz, R. Garcia Fernández, and C. Vega, *J. Chem. Phys.* **122**, 234511 (2005).
- <sup>16</sup>A. J. C. Ladd, B. Moran, and W. G. Hoover, *Phys. Rev. B* **34**, 5058 (1986).
- <sup>17</sup>A. J. H. McGaughey and M. Kaviany, *Adv. Heat Transfer* **39**, 169 (2006).
- <sup>18</sup>G. A. Slack, *Phys. Rev. B* **22**, 3065 (1980).
- <sup>19</sup>R. E. Peierls, *Ann. Phys.* **395**, 1055 (1929).
- <sup>20</sup>P. G. Klemens, in *Solid State Physics*, edited by F. Seitz and D. Turnbull (Academic Press, New York, 1958), Vol. 7.
- <sup>21</sup>S. I. Simdyankin, M. Dzugutov, S. N. Taraskin, and S. R. Elliott, *Phys. Rev. B* **63**, 184301 (2001).
- <sup>22</sup>E. Courtens, M. Foret, B. Hehlen, B. Rufflé, and R. Vacher, *J. Phys.: Condens. Matter* **15**, S1279 (2003).
- <sup>23</sup>R. V. Belosludov, O. S. Subbotin, H. Mizuseki, P. M. Rodger, Y. Kawazoe, and V. R. Belosludov, *J. Chem. Phys.* **129**, 114507 (2008).
- <sup>24</sup>A. Matic *et al.*, *Phys. Rev. Lett.* **93**, 145502 (2004).